The 2013 World Congress on
Advances in Structural Engineering and Mechanics (ASEM13)
Jeju, Korea, September 8-12, 2013

Optimal truss span study for the buckling restrained knee brace truss moment frame

*T.Y. Yang[1] and Yuanjie Li[2]

[1), 2)] *Department of Civil Engineering, University of British Columbia,*
6250 Applied Science Lane, Vancouver, Canada
[1)] *yang@civil.ubc.ca*
[2)] *yuanjieli01@gmail.com*

ABSTRACT

Buckling restrained knee brace truss moment frame (BRKBTMF) is a novel and innovative structural system that utilizes the advantages of open web steel trusses and dedicated structural fuses for seismic applications. Open web steel truss are very economical and effective to span large distance. However, the conventional open web steel trusses (OWST) are not suitable for seismic application due to the lack of ductility and poor energy dissipation capacity. The introduction of buckling restrained knee braces as the dedicated structural fuses can overcome these disadvantages and allow the truss girders to be used efficiently in seismic application. In this paper, a detailed parameter study was conducted to study the performance of the BRKBTMF system with different spans. A prototype building located in Berkley, California, USA, was designed using two truss spans. Nonlinear dynamic analyses were conducted to exam the performance of the structure under the expected maximum credible earthquake shaking intensity. The results show that as the span of the BRKBTMF increased, the truss became less efficient. This results to more steel material to be used in the BRKBTMF, which results to higher initial construction cost. On the other hand, the seismic performance of the BRKBTMF is not significantly affected by truss span.

1. INTRODUCTION

The design philosophy for earthquake engineering applications is shifting towards more resilient design, where the structural damage can be minimized during the maximum credible earthquake shaking. This can be achieved through the use of designated structural fuses, which can protect the rest of the structure from the sudden and infrequent surge of loads created during the earthquake shaking. More importantly, by using of designated structural fuses, the damage can be controlled and the fuses can be easily replaced after the earthquake. This minimizes the repair cost of the

[1)] Assistant Professor
[2)] Graduate Research Assistant

structure, without the need to overly design the structural system to increase the initial construction cost. To achieve this objective, an innovative steel structural system, buckling restrained knee brace truss moment frame (BRKBTMF), is developed. This is a novel steel structural system which utilizes the open web steel truss (OWST) to create a large interior opening and the buckling restrained braces (BRBs) as the designated structural fuses to dissipate the earthquake energy. Previous studies (Wongpakdee et al. 2011 & 2012) have shown that the BRKBTMF is a novel structural system that is suitable for seismic application. In this paper, a detailed parameter study was conducted to optimize the geometric configuration of the BRKBTMF. A prototype building located in Berkeley, California was selected for this study. Finite element models were developed using OpenSees (UCB 2010). Ground motions were selected and scaled to match the site specific seismic hazard in Berkeley and used in the nonlinear dynamic analyses to examine the performance of the structure with different truss spans.

2. SEISMIC DESIGN PROCESS OF THE BRKBTMF

Figure 1 shows the design process of the BRKBTMF. The BRBs were selected as the energy dissipation device. The sizes of the BRBs were selected by equating the energy to be dissipated by the BRBs with the energy generated by the applied loads. After the sizes of the BRBs have been determined, the trusses and the columns were then capacity designed to remain elastic under the maximum axial forces expected in the BRBs and the gravity loads. Details of the design process are given in Wongpakdee et al. (2011).

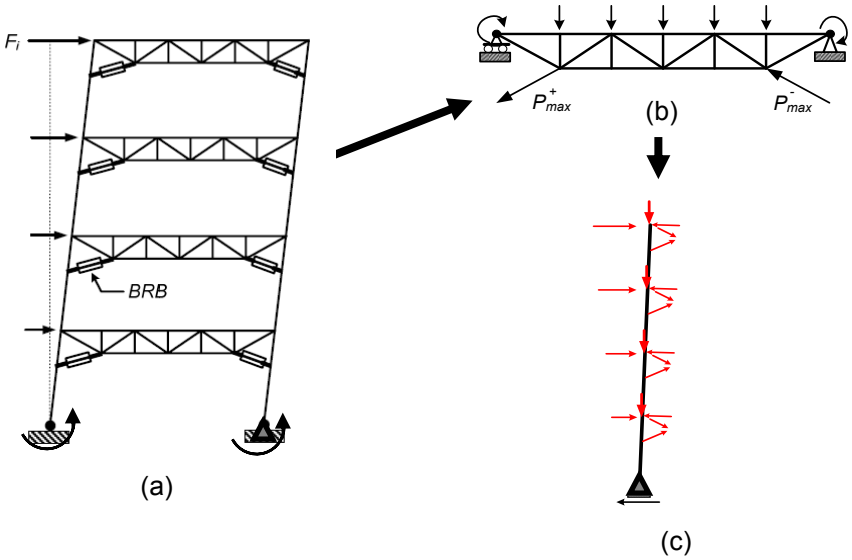

Fig. 1 Design of BRKBTMF: (a) Plastic analysis of the truss frame to determine BRB sizes; (b) capacity design of trusses; and (c) capacity design of columns subjected to BRB and truss forces (Modified from Wongpakdee et al. 2012).

3. DESCRIPTION OF THE PROTOTYPE BUILDING

A prototype office building, as shown in Fig. 2, was selected for this study. The building has a floor plan of 120 ft. x 180 ft. Two types of truss configuration were used. The first type was a 30 ft. truss span which is common in office building (Fig. 2b) and the second configuration was a 60 ft. truss span, which can be used for special building functions, such as conference room or dining hall (Fig. 2c). Note that the BRKBTMF was designed in east-west direction.

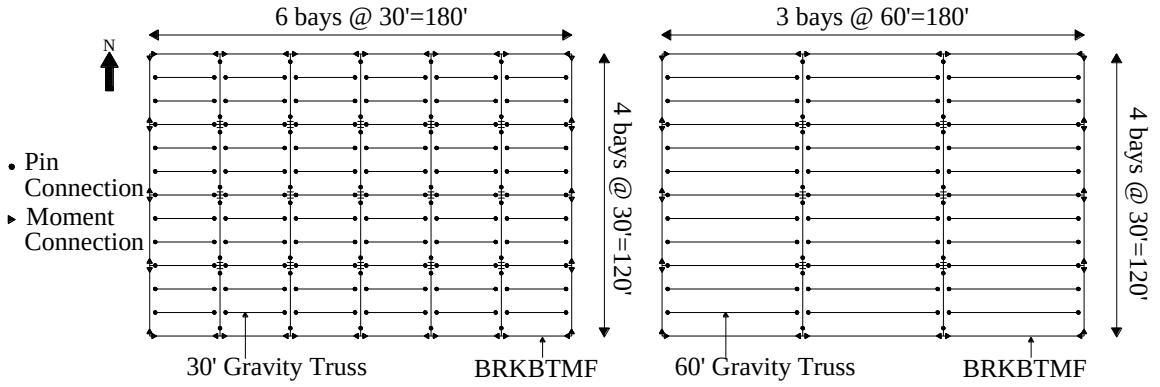

a) Floor plan

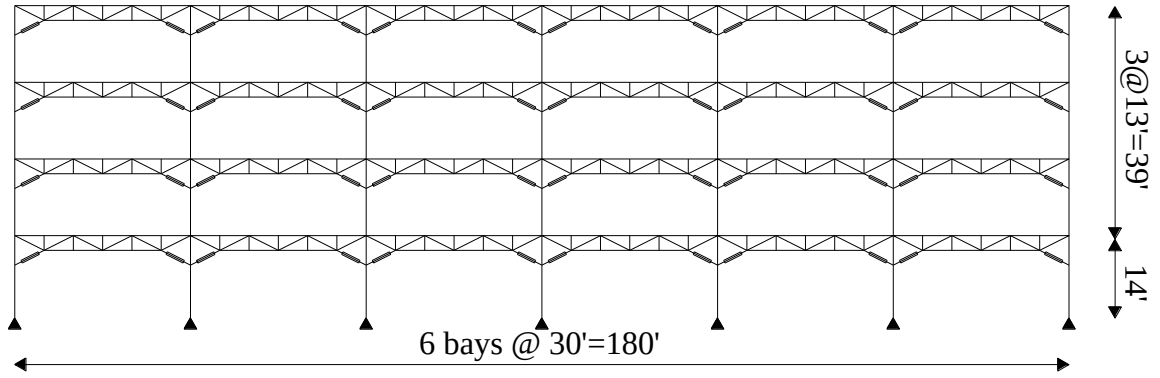

b) Elevation plan (30 ft. configuration)

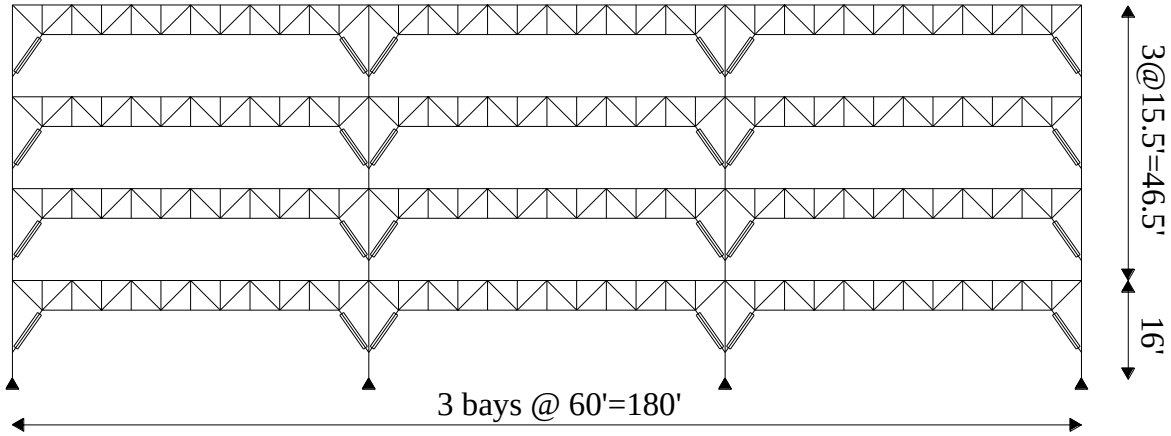

c) Elevation plan (60 ft. configuration)

Fig. 2 Floor and elevation plan of the prototype building

4. OPTIMIZATION DESIGN OF THE OPEN WEB STEEL TRUSSES

To optimize the design of the open web steel truss, a detailed parameter study was conducted. The open web steel truss needs to be capacity designed to remain elastic under the factored gravity load and the maximum force expected in the BRBs. In addition, the vertical deflection of the truss under the service load (unfactored dead load plus live load) needs to be limited to L/240, where L is the clear span length of the truss. The steel truss was assumed to be constructed using three types of member sizes (type A, B and C). Type A was used for all the top and bottom chords. Type B was used for all the vertical members. Type C was used for all the diagonal members. It should be noted that the spacing for the vertical member was arbitrarily selected as 5 ft. In other words, there were a total of 5 and 11 vertical members in each of the 30 ft. and 60 ft. truss configurations, respectively. Equation (1) shows the maximum deflection in the truss under the applied gravity load.

$$\delta = \sum \frac{nNL}{AE} \tag{1}$$

where δ is the deflection at the mid-span of the truss; n are the virtual internal forces under that a unit virtual point force applied at the mid span of the truss. N are the forces in the truss members under the applied gravity load. A, E and L are the area, elastic modulus and length of the corresponding truss members.

By setting the maximum deflection as the L/240, the optimal depth of the truss member can be calculated by minimizing the total usage of the steel material. Note that the loads (factored loads) for strength check is different from the service level deflection check, which uses the unfactored loads. Figure 3 shows the optimal depth of the truss under the gravity load with different spans. The optimal depth of the truss is defined when the design uses the least amount of total steel and still satisfies the strength and deflection limitations. The value α, as presented in Fig. 3, represents the ratio of the live load to the dead load. In most cases, the live load ranges from 0% (α =0) to 300% (α =3) of the dead load. A load combination of 1.2 dead load plus 1.6 live load was used for the strength check, while an unfactored service load of 1.0 dead load plus 1.0 live load was used for the deflection limit check. The result shows that as the ratio α increases, the optimal depth of the truss reduces. In general, the optimal depth of the truss is selected to be about L/12.

Figure 4 shows the total steel usage as a function of the truss depth under a constant gravity load of 1.06 kips/ft. and a variation BRB forces. The constant gravity load of 1.06 kips/ft. was selected to represent the expected factored gravity load to be experienced by the OWST shown in Fig. 2. As expected, as the BRB force increases, the total required steel in the OWST increases. The result shows the total steel usage decreases as the depth of the truss increases. The trend starts to reverse as the depth of the truss goes beyond 10 ft. and 13 ft. for the 30 ft. and 60 ft. configurations, respectively. However, such depth is not practical for buildings construction. Hence the truss depth for the BRKBTMF is limited to L/12.

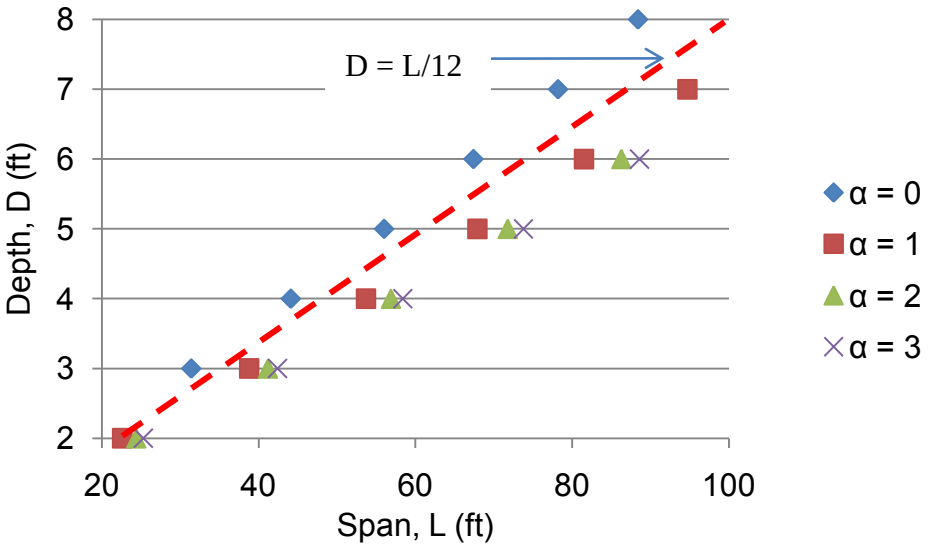

Fig. 3 Optimal depth vs. span

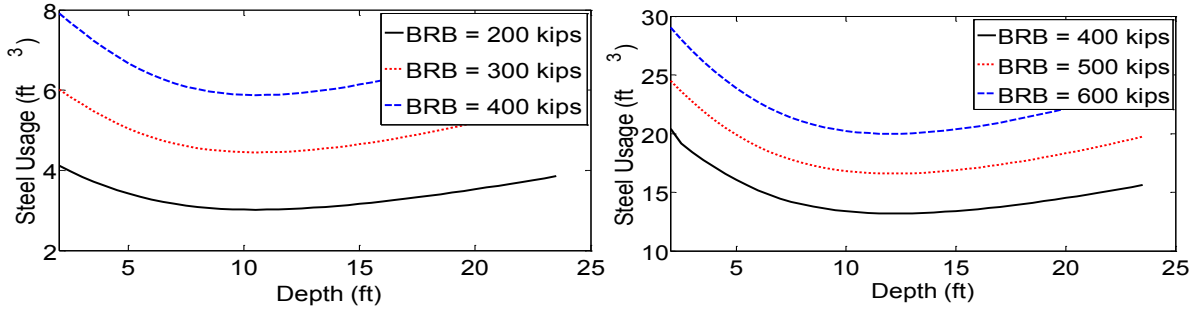

Fig. 4 Steel usage of 30 ft. (left) and 60 ft. (right) truss with various truss depth

Hence a truss depth of 2.5 ft. and 5.0 ft. was selected for the 30 ft. and 60 ft. configurations, respectively. To minimize the total height difference, a fixed clear height of 10.5 ft. was selected for all floors above the 1st floor. The first floor was 14 ft. vs. 16 ft. for the 30 ft. and 60 ft. configurations, respectively. This results to total building heights of 53 ft. and 63 ft. for the 30 ft. and 60 ft. span configurations, respectively. The angles of the BRB were chosen such that the axial strain in the BRBs is identical in the 30 ft. and 60 ft. configurations, under the same inter-story drift. Equation (2) shows the relationship between the axial strain and inter-story drift ratio. The equation is based on the BRKBTMF subassembly shown in Fig. 5. A BRB angle of 63˚ and 35˚ was selected for the 30 ft. and 60 ft. configurations, respectively.

$$\varepsilon = \frac{(D_0 + l_1 / \tan(\alpha)) l_d \theta_p \sin\varphi}{{l_0}^2} \tag{2}$$

where α is the vertical angle between the BRB and the column; D_0 is the depth of truss; l_d is the length of the first diagonal member of the OWST; l_1 is the length of first top

chord, θ_i is the inter-story drift ratio, l_0 is the undeformed length of the BRB; φ is the angle between the column and diagonal chord; and ε is the total axial strain of BRB.

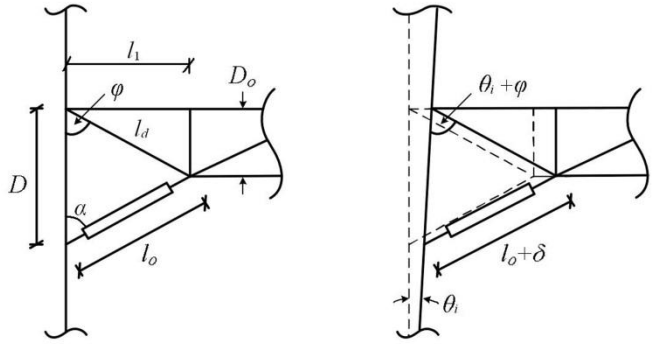

Fig. 5 a) Undeformed geometry on the BRKBTMF subassembly; b) Deform geometry of the BRKBTMF subassembly.

5. GROUND MOTION SELECTION

Ground motions were selected to match site specific maximum credible earthquake (MCE) shaking intensity specified in the U.C. Berkeley Seismic Guidelines (UCB 2003). The ground motions records were selected from the PEER NGA database (2010) and amplitude scaled such that the mean spectrum of the set do not fall below the target spectrum by 10% within the period range from 0.2T (0.2 sec) to 1.5T (1.5 sec) (T is about 1.0 sec for both buildings). The selection of period range is consistent with the ASCE (2010) Section 16.1.3.1 scaling procedure. Figure 6 shows the scaled spectra vs. the target spectrum. Table 1 shows the summary of the ground motions selected.

Tab. 1 Ground motion selected for time history analysis

Year	Event	Station	Magnitude	Scaling Factor
1994	Northridge	Sepulveda VA Hospita	6.69	1.9
1995	Kobe-Japan	Nishi-Akashi	6.90	3.0
1978	Tabas-Iran	Dayhook	7.35	3.7
1999	Chi-Chi-Taiwan	TCU078	7.62	3.4
1976	Friuli-Italy	Tolmezzo	6.50	3.4
1999	Hector Mine	Hector	7.13	3.9
1992	Landers	Lucerne	7.28	4.3
1989	Loma Prieta	WAHO	6.93	2.2
1989	Loma Prieta	Saratoga-Aloha Ave	6.93	4.1
1985	Nahanni-Canada	Site 1	6.76	3.0

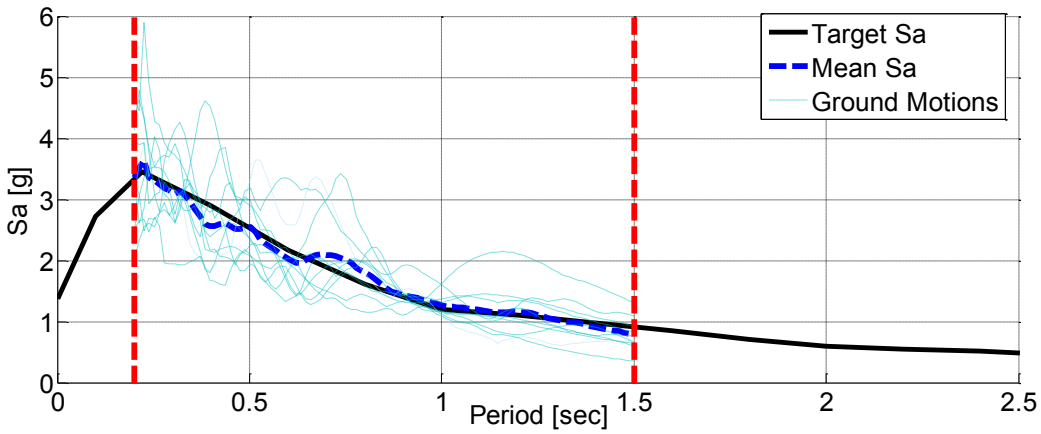

Fig. 6 Ground motions scaled to 2% in 50 years target spectrum.

6. DESIGN RESULT AND STRUCTURAL BEHAVIOR

Tab. 2 Summary of the member sizes

Type	Seismic Columns				BRB (kips)	
	30 ft		60 ft		30 ft	60 ft
Floor	Exterior	Interior	Exterior	Interior		
4	W40X149	W36X160	W40X362	W44X262	227	231
3	W40X149	W36X160	W40X362	W44X262	342	348
2	W40X199	W40X199	W40X362	W44X262	414	420
1	W40X199	W40X199	W40X362	W44X262	449	456
Type	Seismic Truss					
	30ft			60ft		
Floor	Chord	Diagonal	Vertical	Chord	Diagonal	Vertical
4	2MC6X12	2MC6X7	L3.5X3.5X5/16	2MC6X18	2MC6X12	L3.5X3.5X5/16
3	2MC6X15.1	2MC8X8.5	L3.5X3.5X5/16	2MC9X23.9	2MC6X12	L3.5X3.5X5/16
2	2MC6X18	2MC6X12	L3.5X3.5X5/16	2MC10X33.6	2MC6X18	L3.5X3.5X5/16
1	2MC8X20	2MC6X12	L3.5X3.5X5/16	2MC10X33.6	2MC8X20	L3.5X3.5X5/16
Type	Gravity Truss					
	30ft			60ft		
Direct.	Chord	Diagonal	Vertical	Chord	Diagonal	Vertical
E-W	2L2.5X2.5X1/4	2L2X2X3/16	L2X2X1/8	2L3X3X7/16X3/4	2L2.5X2.5X1/4X3/4	L2X2X1/8
N-S	2L5X5X3/8X3/4	2L3.5X3.5X5/16X3/4	L2X2X3/16	2L6X6X5/8	2L6X6X3/8	2L2.5X2.5X3/16

Table 2 shows the comparison of the member sizes for the two configurations considered. Finite element models were developed in Opensees (UCB 2010) and used to compare the structural responses under the maximum credible earthquake shaking intensity. The BRBs were modeled using the truss elements with Steel02 material, the columns were model using the force-based beam-column elements with P-Delta transformation and OWSTs were modeled using the elastic truss elements. Rigid diaphragm was used on each floor by using multiple points constraints. The mass was

assigned accordingly to each node on the floors. The base of the column were pin connection to reduce the possibility to repair the column base after the strong earthquake shaking. Figures 7 and 8 show the median and coefficient of variance (COV) of the peak inter-story drift ratio and the peak floor acceleration obtained from the time history analyses. The response of the truss is very similar between these two configurations. Both configurations have higher drift at the first floor and the drift decreases at higher stories. This is because the bases of the column were pinned. The peak floor acceleration is fairly consistent between these two configurations. The 30 ft. configuration had slightly less drift but more acceleration than the 60 ft. configuration. On the contrary, the COV for drift is slightly higher in the 30 ft. configuration and COV for acceleration is slightly higher in the 60 ft. configuration. In overall, the result shows that the peak floor acceleration and inter-story drift ratio are very similar between these two configurations. Hence, it is concluded that the truss span has minimal effect on the structural responses.

Figure 9 shows the breakdown of the initial construction cost. The initial construction cost was calculated based on the gravity and seismic systems. The result shows that the 60 ft. configurations uses 46% more on gravity truss, 90% more on seismic truss, 10% less in column, 3% less in BRBs as compared to the 30 ft. configuration. The columns and BRBs cost was quite comparable because more force demands were on columns and BRBs in 60 ft. configuration, even though the number to be used was less than 30 ft. configuration. In overall, these results to 26% more in the initial construction cost for the 60 ft. configuration as compared to the 30 ft. configuration.

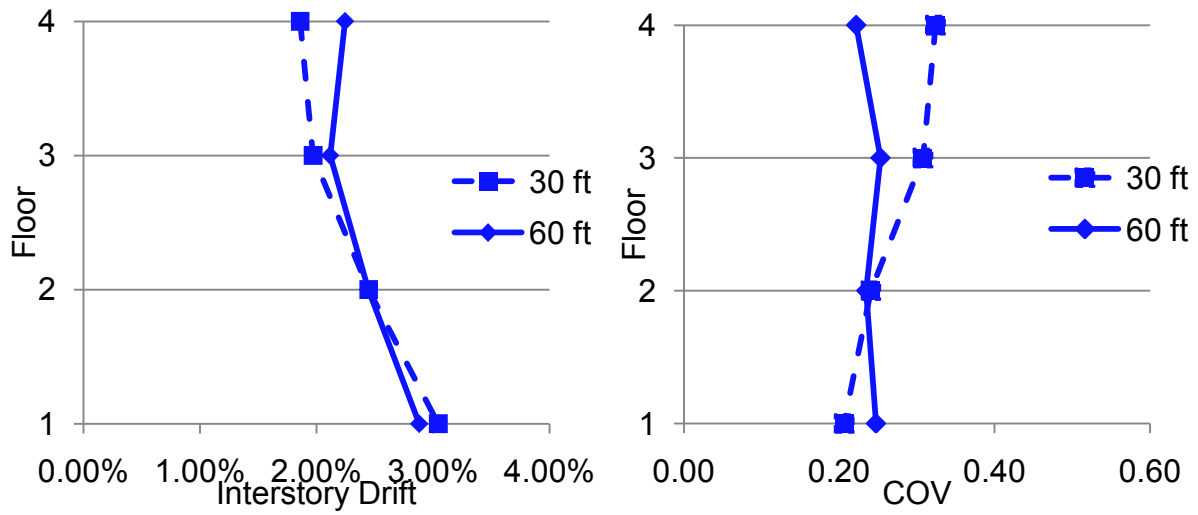

Fig. 7 Median and COV of the peak inter-story drift ratios

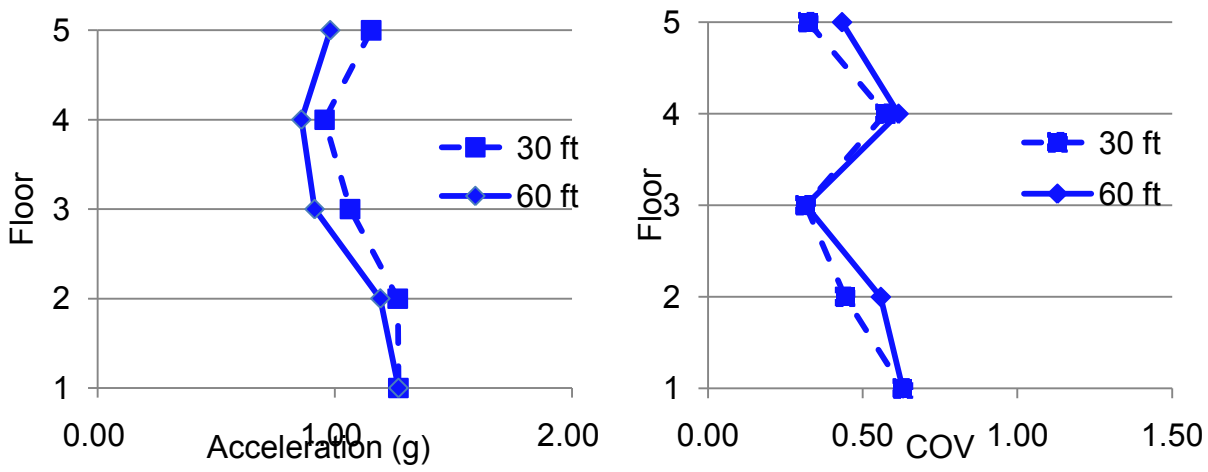

Fig. 8 Median and COV of the peak floor acceleration

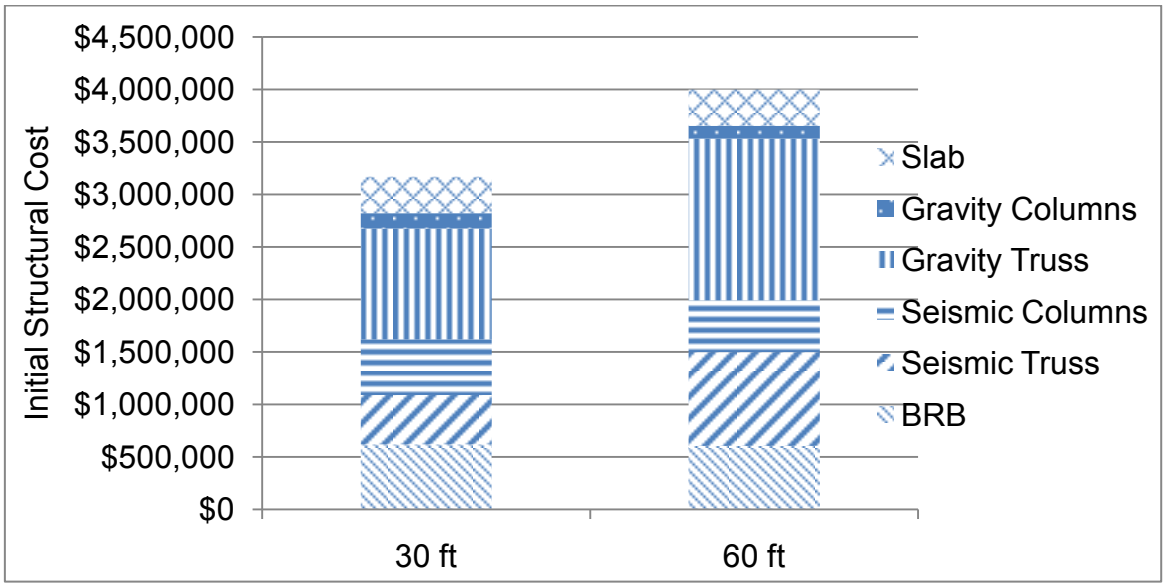

Fig. 9 Cost breakdown for initial structural cost

7. PERFORMANCE EVALUATION STUDY OF THE BRKBTMF

Seismic performance of the BRKBTMF under MCE earthquake shaking intensities was conducted using the state-of-the-art seismic performance assessment procedure outlined in ATC-58 (2008) procedure. Major structural and nonstructural components in the building were grouped into different performance groups. Each performance group consisted of a collection of the building components whose performance was similarly affected by a particular engineering demand parameter (EDP). For examples, the structural components performance group consisted of drift sensitive components, while the non-structural components consisted of acceleration and drift sensitive components. Tab. 3 shows a summary of the performance groups included in this study. Tab. 4 shows a sample of the repair quantities and repair actions required for each of the performance groups in the each damage state.

Multiple damage states were then defined for each performance group. The damage states were established at points along the damage continuum for which significant repair action would likely to be triggered. For each damage state, a damage model (fragility relation) defined the conditional probability of damage being less than or equal to the threshold damage given the value of the engineering demand parameter associated with the performance group. Figure 10 shows samples of fragility relations used to identify the damage state of the performance groups.

The damage state for each performance group was identified using the distribution of the engineering demand parameters presented in Tab. 3 and the fragility curves presented in Fig. 10. For example, Figure 10a shows the fragility curve for the structural elements. If the inter-story drift ratio was 2.5%, there was a 50% chance that the components in that performance group would be damaged (DS2), which means that the components need to be repaired. Using a random number generator between 0 and 1, the damage state for each PG were identified. Details of the damage state identification can be identified in Yang et al. (2009a). Once the damage state of the component was identified, the repair action and the associate repair cost including labor cost could be identified from a look up table as shown in Tab. 4. The total repair cost for the entire building was then calculated by summing the repair cost from each individual item. The process is repeated a large number of times to get a distribution of the total repair cost.

Tab. 3 Summary of performance group

PG No.	PG Name	EDP	EDP description	PG description
1	SH12	du_1	Inter-storey drift between levels 1 and 2	Structural
2	SH23	du_2	Inter-storey drift between levels 2 and 3	
3	SH34	du_3	Inter-storey drift between levels 3 and 4	
4	SH4R	du_4	Inter-storey drift between levels 4 and roof	
5	EXTD12	du_1	Inter-storey drift between levels 1 and 2	Exterior non-structural (displacement sensitive)
6	EXTD23	du_2	Inter-storey drift between levels 2 and 3	
7	EXTD34	du_3	Inter-storey drift between levels 3 and 4	
8	EXTD4R	du_4	Inter-storey drift between levels 4 and roof	
9	INTD12	du_1	Inter-storey drift between levels 1 and 2	Interior non-structural (displacement sensitive)
10	INTD23	du_2	Inter-storey drift between levels 2 and 3	
11	INTD34	du_3	Inter-storey drift between levels 3 and 4	
12	INTD4R	du_4	Inter-storey drift between levels 3 and roof	
13	INTA2	a_2	Total acceleration at level 2	Interior non-structural (acceleration sensitive)
14	INTA3	a_3	Total acceleration at level 3	
15	INTA4	a_4	Total acceleration at level 4	
16	INTAR	a_R	Total acceleration at roof	
17	CONT1	a_g	Ground acceleration	Contents
18	CONT2	a_2	Total acceleration at level 2	
19	CONT3	a_3	Total acceleration at level 3	
20	CONT4	a_4	Total acceleration at level 4	
21	EQUIPR	a_R	Total acceleration at roof	Rooftop equipment

Tab. 4 Sample of repairable components and costs (Yang et al. 2009b)

		Repair quantity				Unit repair cost			
Repair component	Unit	DS1	DS2	DS3	DS4	Min. qua.	Max. cost	Max. qua.	Min. cost
		Structural performance group							
4th floor BRBs	ea	0	24/12	-----	-----	1	$5000/ $8000*	2	$5000/ $8000*
Slab Replacement	ft^2	0	1600	-----	-----	100	$20	1000	$16
		Exterior non-structural performance group (displacement sensitive)							
Erect scaffolding	ft^2	0	6000	6000	-----	1000	$2.5	10000	$2
Precast panels removal	ft^2	0	0	8400	-----	3000	$12	10000	$8
		Interior non-structural performance group (displacement sensitive)							
Door and frame removal	ea	0	8	8	-----	12	$40	48	$25
Carpet Removal	ft^2	0	0	10000	-----	1000	$1.5	20000	$1
		Interior non-structural performance group (acceleration sensitive)							
Furniture removal	ft^2	0	4000	10000	20000	100	$2	1000	$1.25
Ceiling system removal	ft^2	0	0	0	20000	1000	$2	20000	$1.25
		Contents							
papers/books	ft^2	0	0	10000	10000	1000	$0.1	10000	$0.06
Office equipment	ft^2	0	5000	10000	10000	1000	$0.06	10000	$0.04
		Rooftop equipment							
In-situ repair		0	1	1	-----	1	$10,000	2	$10,000
Remove & replace		0	0	1	-----	1	$200,000	2	$200,000

*BRB price for 30 ft. and 60 ft. configuration, respectively.

8. RESULTS OF PERFORMANCE EVALUATION

Figure 11 shows the deaggregation of the median total repair cost of the BRKBTMF with two different truss span configurations. The total repair cost are similar between these two buildings. The cost distribution shows that the nonstructural components damage occupies two-thirds of the total cost, while the rest of repair cost is contributed from the structural damage. The nonstructural components damage is mainly concentrated in the drift sensitive structural component group. Figure 12 shows the cumulative distribution function (CDF) of the total repair cost for these two configurations. The result shows the 30 ft. configuration perform slightly better than the 60 ft. configuration. For example, the expected repair cost (50% probability of exceedance), for the 30 ft. and 60ft. configurations, are 3.9 million and 4.1 million, respectively.

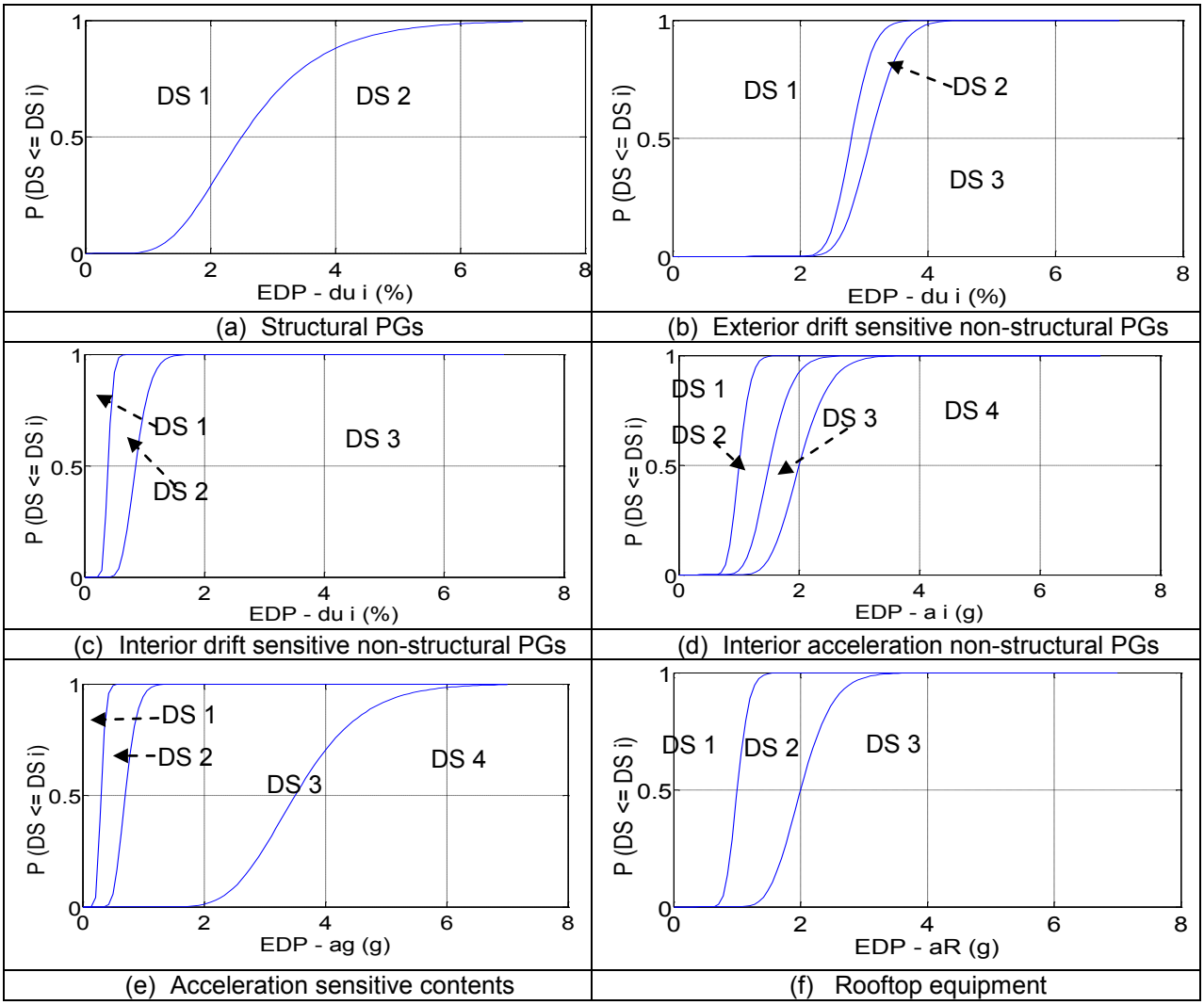

Fig.10 Fragility curves for PGs (Modified from Yang et al. 2009b).

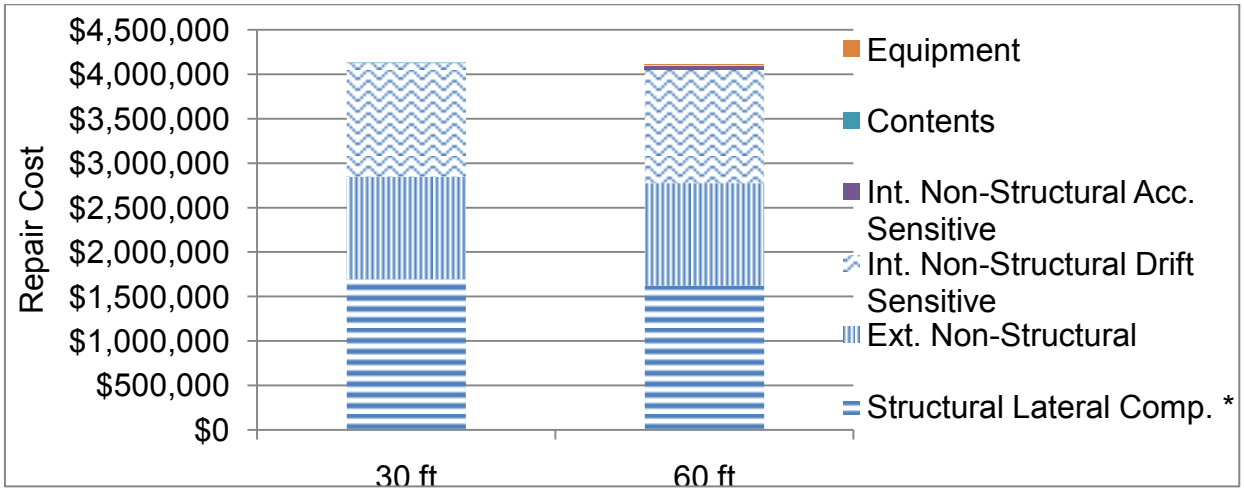

Fig. 11 Cost breakdown total repair cost

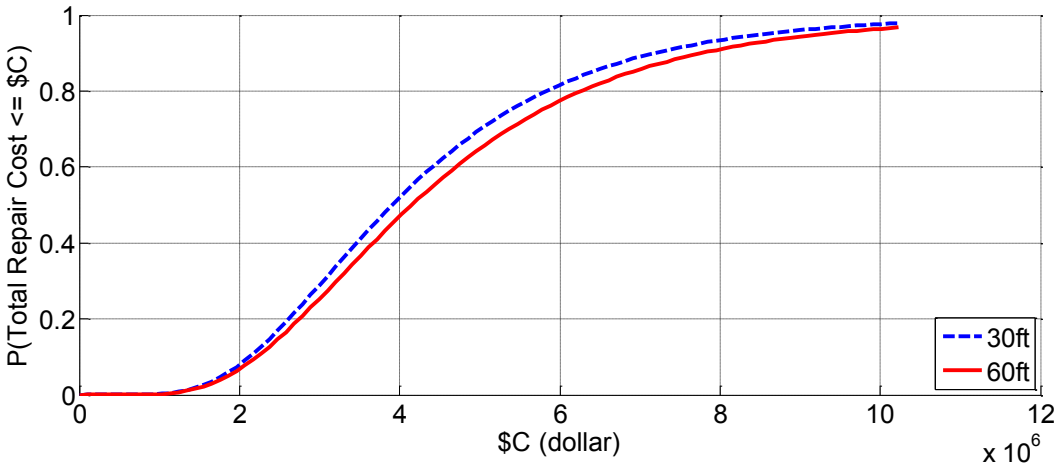

Fig. 12 Cumulative distributed function

9. CONCLUSIONS

Buckling restrained knee brace truss moment frame (BRKBTMF) is a novel steel structural system that utilizes advantages of long span steel truss and buckling restrained braces to create large interior spacing with designated energy dissipation devices for seismic application. In this paper, a prototype building located in Berkeley, California, was designed using the BRKBTMF system. A detailed parameter study was conducted to compare the effectiveness of the BRKBTMF at different truss spans. The following findings were observed from the detailed parameter study.

1) As the ratio of the live load to dead load increase, the optimal depth of the truss decreases. In general, the optimal depth to span ratio for the truss under gravity load is about L/12, where L is the length of the truss span.
2) The optimal design of the seismic truss is highly sensitive to the BRB forces applied at the ends of the seismic truss. In general, as the force in the BRB increases, the total steel usage increases. The depth of the truss has significant impact to the total steel usage. In general, the total steel usage decreases as the depth of the truss increases. However, the optimal depth of the OWST depth under the combined gravity and BRB force are generally too large for building application, hence it is concluded that the OWST depth was selected using the same suggestion as the gravity truss, where the optimal span to depth ratio is approximately 12.
3) The larger truss span could create more flexible and attractive architectural usage for the BRKBTMF. As the length of the truss span increases, the truss became less effective, which results to more initial construction cost. On the other hand, the seismic performance of the BRKBTMF seems not highly affected by the truss span. Hence, it is concluded that the BRKBTMF is an effective structural system for seismic application.

ACKNOWLEDGEMENTS

This work was funded in part by the Natural Sciences and Engineering Research Council of Canada (NSERC) jointly with the Steel Structures Education Foundation (SSEF). The authors would like to acknowledge David MacKinnon of the SSEF for making this project possible. The authors would also like to thank: Prof. S.C. Goel from University of Michigan, Prof. S. Leelataviwat from King Mongkut's University of Technology, and Mr. John D. Hooper from MKA for their valuable advice for this study. Any opinions, findings and conclusion or recommendations expressed in this material are those of the authors and do not necessarily reflect those of the Natural Sciences and Engineering Research Council of Canada or the Steel Structures Education Foundation.

REFERENCES

AISC (2010), "Seismic Provisions for Structural Steel Buildings," American Institute of Steel Construction, ANSI/AISC 341-10, Chicago, IL, USA.

ASCE (2010), "Minimum Design Loads for Buildings and Other Structures," American Society of Civil Engineers Standard, ASCE 7-10, Reston, VA.

Applied Technology Council 58. (2008), Development of next-generation performance-based seismic design procedures for new and existing buildings, Applied Technology Council, <http://www.atcountil.org/atc-59.shtml>.

Balck, C., Makris, N.and Aiken, D. (2004). "Component Testing, Seismic Evaluation and Characterization of Buckling-Restrained Braces," *ASCE Journal of Structural Engineering*, **130**(5), pp. 880-894.

Chao, S-H and Goel, S.C. (2007), "A Seismic Design Lateral Force Distribution Based on Inelastic State of Structures," *Earthquake Spectra*, **23**(3), 547-569.

Goel, S.C. and Chao, S.H. (2008), "Performance-Based Plastic Design: Earthquake-Resistant Steel Structures," International Code Council, USA.

Lopez, W.A., and Sabelli, R., (2004), "Seismic Design of Buckling-Restrained Braced Frames, Steel Tips," Structural Steel Educational Council, California.

OpenSees. (2010), "Open System for Earthquake Engineering Simulation (OpenSees) Framework – Version 2.5", Pacific Earthquake Engineering Research Center, University of California, Berkeley, <http://opensees.berkeley.edu/>.

Pacific Earthquake Engineering Research Center (PEER) Strong Motion Database 2010 BETA version. University of California at Berkeley, <http://peer.berkeley.edu/peer_ground_motion_database>.

UCB. (2003), U.C. Berkeley Seismic Guideline, University of California, Berkeley.

Wongpakdee, N. (2011), “Performance-Based Seismic Design and Evaluation of Buckling Restrained Knee Brace Truss Moment Frames,” Master thesis, Department of Civil Engineering, King Mongkut’s University of Technology Thonburi, Bangkok, Thailand.

Wongpakdee, N.,Leelataviwat, S., Goel, S.C., and Liao, W.C. (2012), “Performance-Based Seismic Design and Evaluation of Buckling Restrained Knee Braced Truss Moment Frames,” *Proceedings, 15th World Conference of Earthquake Engineering,* Lisbon, Portugal, Oct. 13-15, 2012.

Yang, T.Y., Moehle, J.P., Stojadinovic, B. and Der Kiureghian, A. (2009a). “Seismic Performance Evaluation of Facilities: Methodology and Implementation”, *Journal of Structural Engineering, ASCE*, 1146-1154.

Yang, T.Y., Moehle, J.P. and Stojadinovic, B. (2009b). Performance Evaluation of Innovative Steel Braced Frames – PEER Report 2009/103, Pacific Earthquake Engineering Research Center, College of Engineering, University of California, Berkeley.